

# Optimum Design of Vaporizer Fin with Liquefied Natural Gas by Numerical Analysis

Hyo-Min Jeong, Han-Shik Chung\*

School of Mechanical and Aerospace Engineering, the Institute of Marine Industry,  
Gyeongsang National University,

445 Inpyeong-dong, Gyeongsang-namdo 650-160, Korea

Sang-Chul Lee, Tae-Woo Kong, Chung-Seub Yi

Graduate School, Department of Mechanical and Precision Engineering,  
Gyeongsang National University,

445 Inpyeong-dong, Gyeongsang-namdo 650-160, Korea

Generally, the temperature drop under 0°C on vaporizer surface creates frozen dews. This problem seems to increase as the time progress and humidity rises. In addition, the frozen dews create frost deposition. Consequently, heat transfer on vaporizer decreases because frost deposition causes adiabatic condition. Therefore, it is very important to solve this problem. This paper aims to study of the optimum design of used vaporizer at local LNG station. In this paper, experimental results were compared with numerical results. Geometries of numerical and experimental vaporizers were identical. Studied parameters of vaporizer are angle between two fins ( $\Phi$ ) and fin thickness ( $TH_F$ ). Numerical analysis results were presented through the correlations between the ice layer thickness ( $TH_{ICE}$ ) on the vaporizer surface to the temperature distribution of inside vaporizer ( $T_{IN}$ ), fin thickness ( $TH_F$ ), and angle between two fins ( $\Phi$ ). Numerical result shows good agreement with experimental outcome. Finally, the correlations for optimum design of vaporizer are proposed on this paper.

**Key Words :** Liquefied Gas, Vaporizer Fin, Super Low Temperature, Frost Deposition

## Nomenclature

$D_{in}$	: Inside diameter of tube [mm]
$D_o$	: Outside diameter of tube [mm]
$LE_F$	: Length of fin [mm]
$TH_F$ (or $t$ )	: Thickness of fin [mm]
$TH_{ICE}$	: Thickness of frost deposit [mm]
$t/s$	: Ratio of fin thickness to outside curvature interval between fins
$T_{FT}$	: Temperature of fin tip [°C]
$T_{IN}$	: Inner working fluid temperature [°C]

$\Phi$  (or  $s$ ) : Angle between fins [°]

## 1. Introduction

Recently, many Korean researchers have been concentrating on the super low temperature fields due to the increasing demand of the LNG (Liquefied Natural Gas) which has numerous applications such as rapid freezing, cold energy power generation, low temperature refrigeration etc. (Yoon, 2001 ; Nam et al., 2000) LNG consists of CH<sub>4</sub> as the main compound, which is produced by cooling and pressurization process of natural gas. LNG is transported and stored as liquid phase below -162°C from the source country.

LNG must be vaporized to be used as fuel in the industries, home application and so on. In this vaporization process, cold energy in the form of

\* Corresponding Author,

E-mail : hschung@gsnu.ac.kr

TEL : +82-55-640-3185; FAX : +82-55-640-3188

School of Mechanical and Aerospace Engineering, the Institute of Marine Industry, Gyeongsang National University, 445 Inpyeong-dong, Gyeongsang-namdo 650-160, Korea. (Manuscript Received August 25, 2005; Revised February 6, 2006)

latent heat (120 kcal/kg) and sensible heat (80 kcal/kg) are generated. This cold energy can be utilized; however, additional cost of facilities which is needed for vaporization process of LNG reduces its benefit. (Lee et al., 1995, 2001; 2005) Therefore, to utilize cold energy and to develop better vaporizer are very important task.

Generally, the vaporization method of LNG is divided into two types. The first method uses ambient air and the other method uses seawater. The seawater type is used in the coastal LNG station where much heat is required for vaporization process. However, frost deposition from seawater on the surface of vaporizer can cause some problems. Generally, the local LNG station uses air type vaporizer. In the air type vaporizer, the frozen dew is also created by temperature drop (below 0°C) on vaporizer surface. This problem increases as the time progresses and humidity increases. In addition, the frozen dew gradually becomes frost deposit; consequently, heat transfer through vaporizer decreases because frost deposit form adiabatic sheet. (Choi and Chang, 1999) Because of this reason, recent vaporizer system is installed as parallel type; thus, this vaporizer system needs more expensive installation costs and more space.

Yet, LNG vaporizer system must be small, efficient, and easy to operate and maintain. Nowadays, Korea is still at the early phase for super low temperature vaporizer and LNG cold energy utilization technology. Therefore, there are still insufficient practical and theoretical data for super low temperature fields.

The effects of location of fin tube center, fin height, tube thickness, distance between fins about the heat transfer between flue gas and water, and pressure drop of flue gas passing through the fins are investigated numerically by Ereket al. (2005). As one of the results, distance of each fins were found to have significant effect on pressure drop. Tahat et al. (1994) also studied the effects of the heat transfer on distance of each fins, and Sahin et al. (2005) reported on the optimum design parameters of a heat exchanger. A semi-empirical model describing heat and mass transfer on a cold surface in humid air under supersaturated frosting

conditions was carried out and predicted amount of frost collected, frost deposition, heat transfer rate, frost thickness, surface temperature, and other important parameters by Mago and Sherif (2004).

From the previous studies, we can conclude that the important key to solve problems on heat transfer and frost deposition of evaporator are the distance or angle of each fins, length, thickness, material, temperature condition, air humidity and so on.

In this paper, the geometry of vaporizer is star fin-tube type, similar to the vaporizers that are used at the local LNG station. The geometry change of this vaporizer is determined to promote the heat transfer and frost deposition. Accordingly, several parameters such as angle between fins, fin thickness and temperature of working fluid inside vaporizer were adopted in this study. LNG and ambient air was assumed as working fluid inside and outside of vaporizer respectively. Ultimate purpose of this study is to get information of optimal design of vaporizer e.g. star fin-tube by predicting of ice layer thickness on vaporizer surface through numerical analysis. As one of the result, optimal ratio of  $t/s$  as thickness of fin per outside diameter circumference distance between fins was proposed in this paper. Results of this study are expected to be used to improve performance of local LNG station.

## 2. Numerical Method

Utilization of vaporizer in local LNG station is well known in heat changer industry. There are several important parameters to provide adequate vaporization of LNG such as supplied flow-rate of LNG, air condition (humidity and velocity of air), the geometry of fin (width, length, and angle between fins).

For numerical model, CAD was utilized to create surface model; In this study, the numerical models are two-dimensional, and material of fin and tube is pure aluminium. Figure 1 shows the numerical models of vaporizer.  $\phi$  (angle between fins) are 45°, 90°, 120°.  $TH_F$  (the fin thickness) are 2 mm, 4 mm, and 6 mm.  $T_{IN}$  (tempera-

**Table 1** Summary of numerical parameters

Models	Parameters	$\Phi$ (or $s$ )	$TH_F$ (or $t$ )	$T_{IN}$
Model 1		$\Phi=45^\circ (s=1/8\pi D_o)$	2 mm	$-162^\circ\text{C}, -120^\circ\text{C},$
Model 2		$\Phi=90^\circ (s=1/4\pi D_o)$	4 mm	$-80^\circ\text{C}, -40^\circ\text{C},$
Model 3		$\Phi=120^\circ (s=1/3\pi D_o)$	6 mm	$-20^\circ\text{C}$

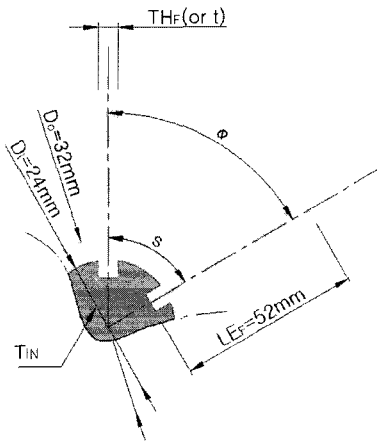


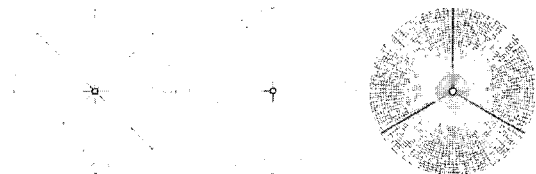
**Fig. 1** Geometry of vaporizer models for numerical analysis

ture of working fluid inside vaporizer) varies from  $-162^\circ\text{C}, -120^\circ\text{C}, -80^\circ\text{C}, -40^\circ\text{C}$ , and  $-20^\circ\text{C}$ . These numerical parameters were summarized in Table 1.

Hexahedral mesh grid was generated by ICEM-CFD software. Numbers of required grid is approximately 40,000. Fig. 2 is the grid system for the calculation area ;

Afterward, STAR-CD (Ađapco Group), a common CFD code, was used for modeling numerical analysis calculation. This two dimensional model of vaporizer does not take account of gravitational effect because vaporizer is modeled in horizontal cross-section. In addition, inner working fluid always keeps on specific temperature, and ambient air temperature is  $20^\circ\text{C}$  at 1.013 bar pressure. This paper uses steady state heat conduction equation since it calculates only base on temperature difference due to absence gravitational effect and mass flow. Main assumption in this study is frost deposit formation only occurs when vaporizer surface temperature below  $0^\circ\text{C}$ .

Figure 3 illustrate a flow chart of the calculation process method in this paper.



(a)  $\Phi=45^\circ$  (b)  $\Phi=90^\circ$  (c)  $\Phi=120^\circ$   
**Fig. 2** Grid system for the calculation zone

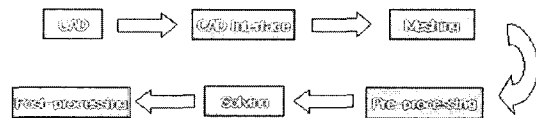


**Fig. 3** Process of calculation

### 3. Numerical Analysis Results and Discussions

Figure 4 shows a vaporizer system in local LNG station. Frost deposit formation between vaporizer fins illustrate in Fig. 4. Meanwhile, results of numerical study on frost deposit thickness and temperature of fin tip were illustrated in Fig. 5. Table 2 summarizes the overall results of this study.

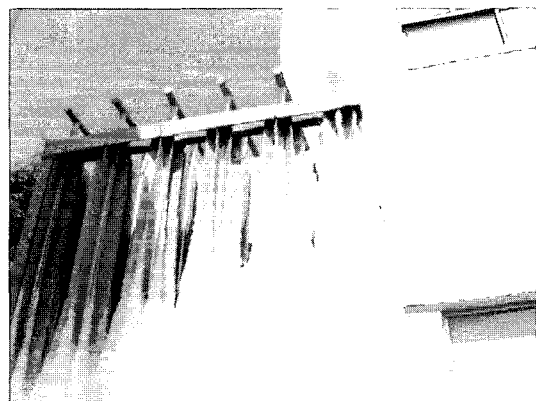


**Fig. 4** Actual photograph on frost deposit of the general vaporizer

**Table 2** Summary of numerical analysis results

$T_{IN}$	$t/s$	$TH_{ICE}$	$T_{FT}$	$\Phi$	$TH_F$
-162	0.0637	30.5	-153	120	2
	0.0849	36.77	-154.9	90	2
	0.1274	33.26	-157	120	4
	0.1699	56	-155.7	45	2
	0.1699	38.8	-158.2	90	4
	0.1911	34.52	-158.6	120	6
	0.2548	40.65	-159.3	90	6
	0.3397	59.93	-158.5	45	4
0.5096	63.45	-159.5	45	6	
-120	0.0637	24.27	-113.9	120	2
	0.0849	29.82	-114.3	90	2
	0.1274	24.97	-116.5	120	4
	0.1699	48.89	-115.3	45	2
	0.1699	30.75	-117.2	90	4
	0.1911	26.98	-117.5	120	6
	0.2548	31.65	-118	90	6
	0.3397	51.2	-117.4	45	4
0.5096	54.48	-118.2	45	6	
-80	0.0637	15.38	-75.64	120	2
	0.0849	18.03	-76.24	90	2
	0.1274	16.21	-77.62	120	4
	0.1699	41.81	-76.75	45	2
	0.1699	19.92	-78.1	90	4
	0.1911	18.15	-78.31	120	6
	0.2548	21.24	-78.65	90	6
	0.3397	43.66	-78.21	45	4
0.5096	45.31	-78.74	45	6	
-40	0.0637	6.3	-37.5	120	2
	0.0849	7.375	-37.77	90	2
	0.1274	6.78	-38.64	120	4
	0.1699	27.83	-38.1	45	2
	0.1699	8.16	-38.9	90	4
	0.1911	8.06	-39.04	120	6
	0.2548	8.52	-39.2	90	6
	0.3397	30.87	-38.95	45	4
0.5096	32.85	-39.27	45	6	
-20	0.0637	2.77	-18.37	120	2
	0.0849	3.01	-18.54	90	2
	0.1274	3.07	-19.12	120	4
	0.1699	9.45	-18.75	45	2
	0.1699	3.36	-19.28	90	4
	0.1911	3.37	-19.37	120	6
	0.2548	3.75	-19.49	90	6
	0.3397	14.82	-19.31	45	4
0.5096	20.3	-19.52	45	6	

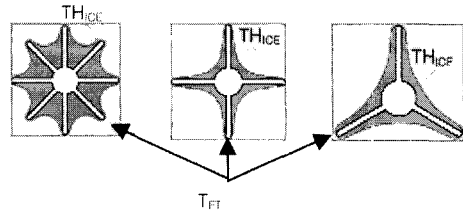


**Fig. 5** A part of the calculated thickness of frost deposit and tip temperature of fin on each vaporizer

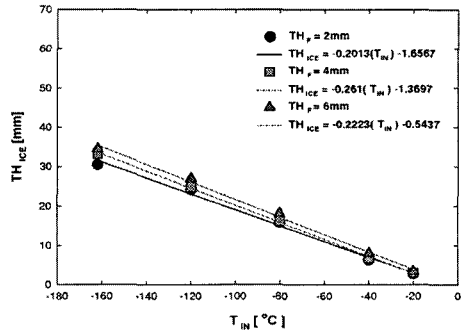
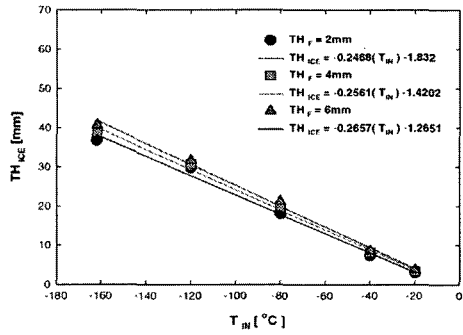
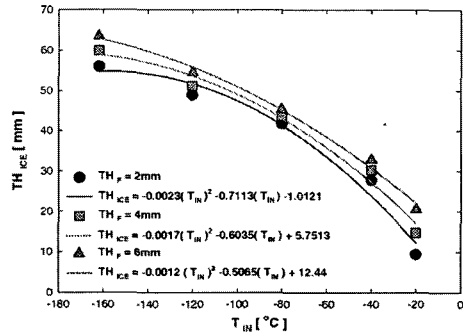


**Fig. 6** Thickness of frost deposit according to variation of fin thickness and inner temperature on vaporizer with each other different angle between fins

Figure 6 shows the  $TH_{ICE}$  in relation with  $TH_F$ ,  $T_{IN}$  temperature, and  $T_{IN}$  at  $\Phi=45^\circ, 90^\circ, 120^\circ$ . As shown on the Fig. 6, the thickness of  $TH_{ICE}$  decreases when the  $\Phi$  and the  $T_{IN}$  fluid temperature increase, yet  $TH_{ICE}$  increases as vaporizer fin ( $TH_F$ ) thickens.

However, by comparing the ice thickness difference ( $\Delta TH_{ICE}$ ) of frost deposit among various  $TH_F$ , in case of  $\Phi=45^\circ$ , the lowest  $\Delta TH_{ICE}$  occur at  $T_{IN}=-80^\circ\text{C}$ ,  $\Delta TH_{ICE}$  will increase if working fluid temperature ( $T_{IN}$ ) is lower or higher than  $-80^\circ\text{C}$ . On the other hand, thickness difference of frost deposit of the  $\Phi=90^\circ$  and  $\Phi=120^\circ$  gradually decrease by temperature growth of inner working fluid. Therefore, for  $\Phi>90^\circ$ , as  $T_{IN}$  temperature increases, variation of  $TH_F$  contribute less effect to the  $TH_{ICE}$ . Here, we can find that vaporizer model with  $TH_F=2\text{ mm}$  generates the thinnest frost deposits. In addition, the fin angle ( $\Phi$ ) has more influence to frost deposition than fin thickness ( $TH_F$ ). The correlation of  $TH_{ICE}$  and  $T_{IN}$  is presented in Table 3.

Figure 7 shows the correlation between  $TH_{ICE}$  and  $T_{IN}$  to  $t/s$  ratios. In this study, there are two conditions that have same  $t/s$  ratio ; one is vaporizer with  $\Phi=45^\circ$  and  $TH_F=2\text{ mm}$ . the other is vaporizer with  $\Phi=90^\circ$  and  $TH_F=4\text{ mm}$ . Both of them have  $t/s$  ratio=0.1699. However, based on numerical results, these two models have different  $TH_{ICE}$ .  $TH_{ICE}$  of vaporizer with  $\Phi=90^\circ$  and  $TH_F=4$  was less than that of vaporizer with  $\Phi=45^\circ$  and  $TH_F=2\text{ mm}$ . This results can be known

**Table 3** Correlation equations of ice layer thickness according to inner temperature variation of vaporizer

$t/s$	Correlation Eq.	$\Phi$	$TH_F$
0.0637	$TH_{ICE} = -0.2013(T_{IN}) - 1.6567$	120	2
0.0849	$TH_{ICE} = -0.2468(T_{IN}) - 1.832$	90	2
0.1274	$TH_{ICE} = -0.261(T_{IN}) - 1.3697$	120	4
0.1699	$TH_{ICE} = -0.023(T_{IN})^2 - 0.7113(T_{IN}) - 1.0121$	45	2
0.1699	$TH_{ICE} = -0.2561(T_{IN}) - 1.4202$	90	4
0.1911	$TH_{ICE} = -0.2223(T_{IN}) - 0.5437$	120	6
0.2548	$TH_{ICE} = -0.2657(T_{IN}) - 1.2651$	90	6
0.3397	$TH_{ICE} = -0.0017(T_{IN})^2 - 0.6035(T_{IN}) + 5.7513$	45	4
0.5096	$TH_{ICE} = -0.0012(T_{IN})^2 - 0.5065(T_{IN}) + 12.44$	45	6

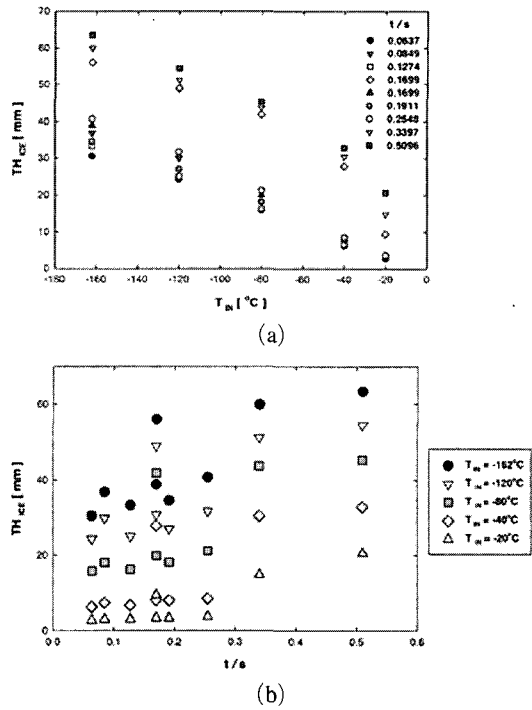


**Fig. 7** Thickness of frost deposit of vaporizer surface according to the increase of working fluid temperature and ratio of  $t/s$

in Fig. 7(a).

Furthermore, it is found that  $t/s=0.1699$  ( $\Phi=45^\circ$  and  $TH_F=2\text{ mm}$ ),  $t/s=0.2584$  ( $\Phi=45^\circ$  and  $TH_F=4\text{ mm}$ ) and  $t/s=0.5096$  ( $\Phi=45^\circ$  and  $TH_F=6\text{ mm}$ ) generate relatively thicker frost deposit ( $TH_{ICE}$ ) than  $\Phi=90^\circ$  and  $\Phi=120^\circ$  models. By these

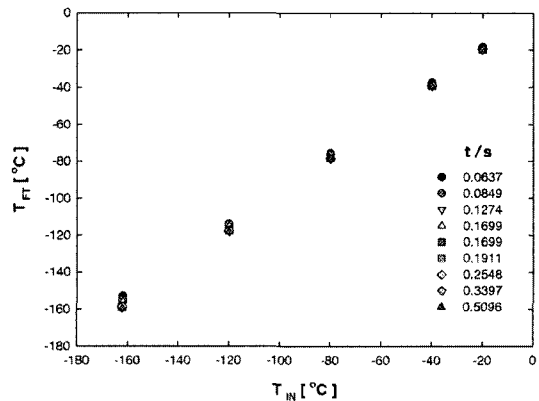


**Fig. 8** Fin tip temperature distributions of vaporizer fin according to the increase of working fluid temperature and ratio of  $t/s$

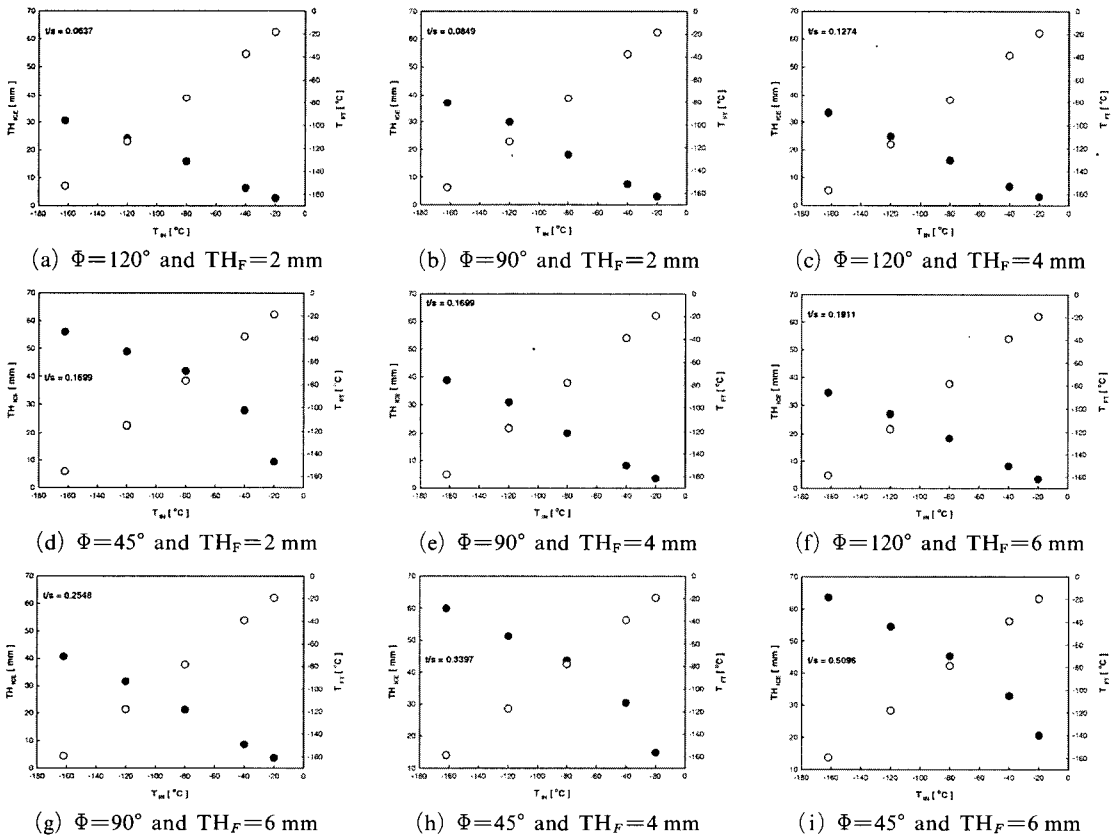
reasons, we have to avoid vaporizer geometry that has  $t/s$  ratio=0.1699, 0.2584 and 0.5096. Figure 8 shows the final temperature distributions of  $T_{FT}$  as function of  $T_{IN}$  and  $t/s$  ratio. Increasing  $T_{FT}$  with increasing temperature of  $T_{IN}$  is understandable. Temperature of  $T_{FT}$  obviously will increase as  $T_{IN}$  temperature increases. In addition, the temperature difference at fin tip by the variation of  $t/s$  ratio decrease as the  $T_{IN}$  increases. Temperature of  $T_{FT}$  at  $t/s=0.0637$  shows the highest temperature. Correlation between  $T_{FT}$  with  $T_{IN}$  was presented on Table 4.

Figure 9 shows comparison between  $TH_{ICE}$  and  $T_{FT}$  as function of  $T_{IN}$  at each  $t/s$  ratio. As the  $T_{FT}$  temperature increases,  $TH_{ICE}$  decreases and  $T_{FT}$  increases.  $T_{FT}$  shows similar temperature distributions by variation of  $t/s$  ratio. On the contrary,  $TH_{ICE}$  is more differ by  $t/s$  variation. Quantitative values of graph in Fig. 9 is shown in Table 1.

As shown in Table 1, we know that  $t/s=0.1699$  ( $\Phi=45^\circ$  and  $TH_F=2$  mm),  $t/s=0.2584$  ( $\Phi=45^\circ$  and  $TH_F=4$  mm) and  $t/s=0.5096$  ( $\Phi=45^\circ$  and  $TH_F=6$  mm) relatively have thicker frost deposit ( $TH_{ICE}$ ) and lower  $T_{FT}$  temperature compare to

**Table 4** Correlation equations of fin tip temperature according to inner temperature variation of vaporizer

$t/s$	Correlation Eq.	$\Phi$	$TH_F$
0.0637	$T_{FT}=0.9493(T_{IN})+0.4412$	120	2
0.0849	$T_{FT}=0.9595(T_{IN})+0.6287$	90	2
0.1274	$T_{FT}=0.9713(T_{IN})+0.2035$	120	4
0.1699	$T_{FT}=0.9645(T_{IN})+0.4814$	45	2
0.1699	$T_{FT}=0.9783(T_{IN})+0.2349$	90	4
0.1911	$T_{FT}=-0.9805(T_{IN})+0.1873$	120	6
0.2548	$T_{FT}=0.9846(T_{IN})+0.1745$	90	6
0.3397	$T_{FT}=0.9802(T_{IN})+0.2588$	45	4
0.5096	$T_{FT}=0.9859(T_{IN})+0.1647$	45	6



**Fig. 9** Comparison of thickness for frost deposit with fin tip temperature for working fluid

others. Fig. 9 also verifies this result. Therefore, these geometries are not recommended for vaporizer design.

Among the remaining vaporizer design, with presence of frost deposit, optimal geometry for vaporizer design is  $t/s=0.0637$  ( $\Phi=120^\circ$  and  $TH_F=2$  mm), this assessment only consider frost deposit ( $TH_{ICE}$ ) and fin tip temperature ( $T_{FT}$ ). However, it say that this geometry shows relatively poor heat transfer rate compared to other geometries when frost deposit is absent. This conclusion cannot be applied for condition without frost deposit because this numerical analysis results was simulated with the presence frost deposit.

Geometry  $t/s=0.849$  ( $\Phi=90^\circ$  and  $TH_F=2$  mm), is estimated as the optimum geometry for vaporizer which operates in two condition, with or without presence of frost deposit. This geometry has more transfer area more than  $t/s=0.0637$ , shows better heat transfer performance. This study recommends  $t/s=0.849$  ( $\Phi=90^\circ$  and  $TH_F=2$  mm) as the optimum vaporizer design, which regard as the most suitable vaporizer design. In addition, the vaporizer geometries could be changed according to the field condition in the range of  $t/s$  ratios of this study, excluding  $t/s=0.1699$  ( $\Phi=45^\circ$  and  $TH_F=2$  mm),  $t/s=0.2584$  ( $\Phi=45^\circ$  and  $TH_F=4$  mm) and  $t/s=0.5096$  ( $\Phi=45^\circ$  and  $TH_F=6$  mm).

#### 4. Comparison Between Numerical Analysis and Experiment

The experimental study has been performed to verify numerical analysis results. Numerical method was calculated by the unsteady state heat conduction, since the real experiment also occurs in the unsteady state.

Figure 10 shows the physical model of vaporizer which has ratio of  $t/s=0.849$  ( $\Phi=90^\circ$  and  $TH_F=2$  mm). In contrast to the numerical analysis, the experimental study used liquefied nitrogen ( $LN_2$ ) as inner working fluid of vaporizer.  $LN_2$  has a normal boiling point  $-196^\circ\text{C}$  at 1.013 bar pressure. Therefore, to imitate the temperature condition similar to the numerical analysis working fluid, nitrogen temperature was constantly

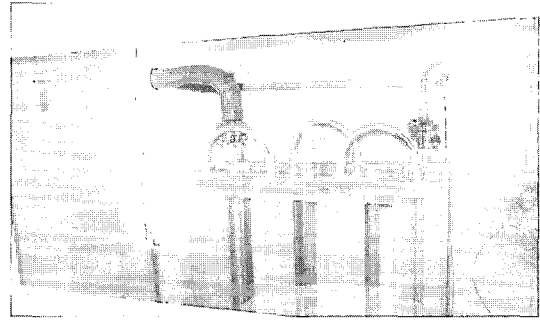


Fig. 10 Photograph of experimental setup for verification of numerical analysis

maintained at  $-162^\circ\text{C}$  by controlling a heating coil. The testing room temperature is  $20^\circ\text{C}$  and air humidity is 43%. The material of physical vaporizer is A6063S, which has excellent heat conductivity. T-type thermocouple was installed at fin tip to get  $T_{FT}$  temperature during the experiment.

Numerical analysis of the heat conduction equation of unsteady state was calculated by using boundary condition written above and did not consider air humidity. In addition, the vaporizer material for numerical analysis is assumed as pure aluminum. Because numerical analysis for verification is unsteady state, time interval of calculation was set every 0.0001 s by using fully implicit scheme and calculation was performed every 8 sec.

Figure 11 shows temperature distributions of fin tip ( $T_{FT}$ ) by the experiment and numerical method during specific period. The experimental result takes about 6.5 s to reach  $0^\circ\text{C}$ , on the other hand the numerical result takes 5 s. The heat transfer prior to frost deposit formation was rapidly occurred. However, once the frost establishes on the surface area of heat transfer e.g. fin surface, heat transfer rate will decrease.

Time difference between the experimental and numerical results to reach  $0^\circ\text{C}$  is 1.5 sec. Although numerical result reaches freezing condition faster than experimental result, the pattern of the temperature distribution of the numerical result is relatively equivalent to the experimental result, and this can be verified by comparing the graph in Fig. 11.

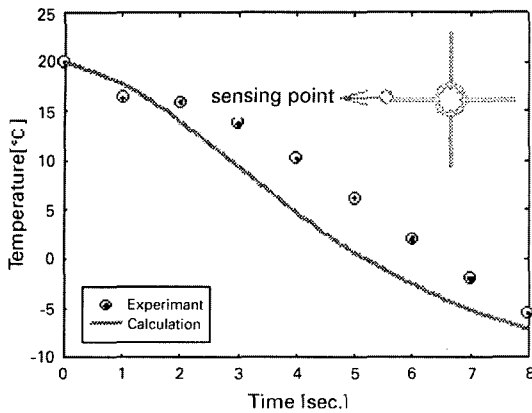


**Fig. 11** The fin tip temperature distribution of the experiment and calculation according to time variation at the working fluid temperature of  $-162^{\circ}\text{C}$

## 5. Conclusions

Numerical analysis for obtaining optimum design of LNG vaporizer and the predicting frost deposit formation on vaporizer fin has been carried out. The results of numerical analysis are:

(1) Without frost deposit presence, increasing of fin thickness ( $TH_F$ ) and decreasing of angle between fins ( $\Phi$ ) will promote heat transfer rate on vaporizer due to enlargement of heat transfer area, however, when frost deposit grows up, heat transfer rate is predicted to decrease by increasing of the ice layer thickness.

(2) Considering the frost thickness ( $TH_{ICE}$ ) and temperature of fin tip ( $T_{FT}$ ),  $t/s=0.849$  ( $\Phi=90^{\circ}$  and  $TH_F=2$  mm) is recommend as the optimum vaporizer geometry. Because it shows optimum heat transfer rate with and without presence of frost deposit.

(3)  $t/s$  as ratio of fin thickness ( $TH_F$ ) to angle between fins ( $\Phi$ ) was defined in this paper. Quantitative values of the frost deposit thickness ( $TH_{ICE}$ ) and fin tip temperature ( $T_{FT}$ ) data according to working fluid temperatures ( $T_{IN}$ ) and  $t/s$  ( $0.0637 \leq t/s \leq 0.5096$ ) were obtained. This numerical data is valid for vaporizer tube with outside diameter  $D_o=32$  mm and the inside diameter  $D_{in}=24$  mm.

(4) The correlation of the frost thickness ( $TH_{ICE}$ ) and fin tip temperature ( $T_{FT}$ ) according to work-

ing fluid temperature ( $T_{IN}$ ) variation were proposed. The numerical result was verified by comparing with experimental result. Numerical result shows good agreement with experimental outcome.

## Acknowledgments

This work was supported by the Program for the Training of Graduate Students in Regional Innovation which was conducted by the Ministry of Commerce, Industry and Energy of Korean Government, and the Korean Institute of Environmental Science and Technology (KIEST) and NURI project, the authors gratefully appreciate for the support.

## References

- Adapco Group, C. D., "STAR-CD METHODOLOGY" Computational Dynamics Ltd., Ver 3. 15.
- Choi, K. I. and Chang, G. M., 1999, "Influence of Formation in a Cryogenic Nitrogen-Ambient Air Heat Exchanger on Power Generation Cycle Utilizing Cold Energy," *Proceeding of the SAREK*, pp. 95~100.
- Erek, A., Ozerdem, B., Bilir, L. and Ilken, Z., 2005, "Effect of Geometrical Parameters on Heat Transfer and Pressure Drop Characteristics of Plate Fin and Tube Heat Exchangers," *Applied Thermal Engineering*, Vol. 25, pp. 2421~2431.
- Lee, G. S., Chang, Y. S. and Ro, S. T., 1995, 2001, "Thermodynamic Analysis of the Extraction Process and the Cold Energy Utilization of LNG," *Korean Journal of Air-Conditioning and Refrigeration Engineering*, Vol. 7, No. 1, pp. 120~131.
- Lee, S. C. et al., 2005, "The Experimental Study on the Thermal Characteristics on Cryogenic Heat Exchange System with Various Parameters," *Proceedings of the International Conference on the Cooling and Heating Technology*, Vol. 1, pp. 11~17.
- Margo, Mago, J. P., and Sherif, S. A., 2004, "Frost Formation and Heat Transfer on a Cold Surface in Ice Fog," *International Journal of*



*Refrigeration*, Vol. 28, pp. 538~546.

Nam, S. C., Lee, S. C. and Park, B. D., 2000, "Performance of Evaporation Heat Transfer Enhancement and Pressure Drop for Liquid Nitrogen," *Trans. of KSME (B)*, Vol. 24, No. 3, pp. 363~372.

Sahin, B., Yakut, K. and Kotcioglu, I., 2005, "Optimum Design Parameters of a Heat Ex-

changer," *Applied Energy*, Vol. 82, pp. 90~106.

Tahat, M. A., Babus'Haq, R. F. and Probert, S. D., 1994, "Thermal Performance of a Fin-Fin Arrays and Performance," *Applied Energy*, Vol. 48, pp. 419~442.

Yoon, J. I., 2001, "Trtips of Research and Development of LNG Cold," *Journal of the KSPSE*, Vol. 5, No. 4, pp. 5~10.